Journal of Chromatography, 637 (1993) 19–28
Elsevier Science Publishers B.V., Amsterdam

CHROM. 24 913

Study of band broadening in enantioselective separations using microcrystalline cellulose triacetate

II. Frontal analysis

Andreas Seidel-Morgenstern

Institute of Technical Chemistry, Technical University, W-1000 Berlin (Germany)

Stephen C. Jacobson

Division of Analytical Chemistry, Oak Ridge National Laboratory, Oak Ridge, TN 37831-6142 (USA)

Georges Guiochon*

Division of Analytical Chemistry, Oak Ridge National Laboratory, Oak Ridge, TN 37831-6142 (USA) and Department of Chemistry, University of Tennessee, Knoxville, TN 37996-1501 (USA)

(First received September 9th, 1992; revised manuscript received January 25th, 1993)

ABSTRACT

Frontal analysis is classically used to measure adsorption isotherms, and in this work the isotherms of Tröger's base were determined on microcrystalline cellulose triacetate with ethanol as solvent at 30, 40 and 50°C for the (−)-enantiomer and at 30°C for the (+)-enantiomer. The isotherms of the first eluted (−)-enantiomer are described satisfactorily by the Langmuir equation at all temperatures. In contrast, the isotherm of the longer retained (+)-enantiomer possesses a pronounced inflection point and can be described by a quadratic isotherm equation. However, besides supplying information about the adsorption equilibrium, frontal analysis data can be used to determine kinetic parameters. Using the equilibrium-dispersive model of chromatography, the apparent axial dispersion coefficient was derived by fitting the breakthrough curve for each concentration step. The values are in general agreement with those obtained from the classical determination of the efficiency of elution profiles under linear conditions. However, the apparent dispersion coefficient determined from frontal analysis depends on the concentration.

INTRODUCTION

The equilibrium isotherm is the most important prerequisite for modeling separation processes in liquid chromatography. In the present state of our understanding of phase equilibria, this information can be obtained only on the basis of experimental investigations. The different methods of adsorption isotherm measurements have been reviewed recently by Katti and Guiochon [1]. For chromatographic systems that have low efficiency, frontal analysis (FA) is the most suitable method.

* Corresponding author. Address for correspondence: Department of Chemistry, University of Tennessee, Knoxville, TN 37996-1501, USA.

0021-9673/93/$06.00

Besides isotherms, kinetic parameters must also be known, because of their effect on band broadening. To study mass transfer and adsorption kinetics, different approaches are available. Most often, small injections are made at different flow rates, and their profiles are analyzed on the basis of the Van Deemter plot or of the theory of statistical moments. These measurements are carried out in the linear range of the adsorption isotherms. This permits the study of the contributions of the different kinetic phenomena.

It has been demonstrated for all chromatographic systems that we have studied that the different possible kinetic effects, *e.g.*, axial dispersion in the bulk phase, diffusion through a laminar boundary layer around the solid particles, different types of intraparticle mass transfer resistances and adsorption–desorption kinetics, can be satisfactorily combined into an apparent dispersion coefficient [1–5]. This coefficient can be conveniently determined from the retention time and band width of injections of small sample sizes. However, when applying this method one is not assured that the apparent dispersion coefficient remains independent of the concentration.

The purpose of this work was a further analysis of experimental frontal analysis data that were collected to determine adsorption isotherms. A value of the apparent dispersion coefficient was determined for each of the breakthrough curves measured, thus covering a wide concentration range. The results are compared with those of the analysis of elution band profiles, and the dependence of this kinetic parameter on the average concentration can be studied.

Recently we reported an experimental investigation of the adsorption isotherms of Tröger's base enantiomers (TB) on swollen microcrystalline cellulose triacetate (CTA) from ethanol solutions [6]. CTA is an important stationary phase, widely used for enantioselective separations by preparative chromatography. Many racemates have been successfully separated with this material [7]. CTA has good mechanical properties and is relatively inexpensive compared with other chiral phases. TB is a classical racemate [8]. In our recent studies its unusual retention behavior on CTA observed by several workers was explained as the consequence of different isotherm shapes for the two TB enantiomers [5,6]. Whereas the isotherm of the less retained (−)-enantiomer could be described by a Langmuir isotherm equation, the isotherm of the longer retained (+)-enantiomer exhibited an inflection point and a quadratic isotherm equation was needed for its description.

THEORY

Frontal analysis

In FA, successive step changes in the eluent composition at the column inlet are performed. Solving the integral mass balance equation at each breakthrough curve gives one point of the isotherm. The amount adsorbed during each step of an FA run is obtained from

$$t_R = t_0\left[1 + F \cdot \frac{q(C_E) - q_0}{C_E - C_0}\right] \quad (1)$$

where $q_0 = q_0(C_0)$ is the amount adsorbed at equilibrium before the step change from concentration C_0 to concentration C_E at column inlet, $q(C_E)$ is the amount adsorbed at equilibrium after the step change, t_0 is the retention time of a non-retained component and F is the phase ratio. Eqn. 1 allows the determination of the point of the isotherm, $q(C_E)$, from the retention time of the breakthrough front, t_R.

Owing to the self-sharpening of the breakthrough fronts, the concentration steps ought to be positive for the determination of isotherms of the Langmuir type. If the curvature of the isotherm is opposite, decreasing concentration steps should be used.

Adsorption isotherms

Simple considerations of statistical thermodynamics result in the following general adsorption isotherm equation [9,10]:

$$q = q_s \cdot \frac{C(b_1 + 2b_2C + 3b_3C^2 + \cdots + nb_nC^{n-1})}{1 + b_1C + b_2C^2 + b_3C^3 + \cdots + b_nC^n} \quad (2)$$

where the product nq_s is the saturation capacity of the adsorbent and the temperature dependent coefficients b_i are related to the partition functions for an individual molecule adsorbed on the ith monomolecular layer [9].

The first- ($b_{2+} = 0$) and second-order ($b_{3+} = 0$) equations of the general type proposed in eqn. 2 are the Langmuir and the quadratic isotherm equations, respectively [10]. The adsorption of only one molecule on each adsorption site of the saturated monolayer is assumed in the former model, but that of two molecules in the latter.

In a recent study, the applicability of the Langmuir and the quadratic isotherm equations for describing the adsorption isotherms of the (−)- and (+)-enantiomers of TB on CTA was shown [5,6].

Equilibrium dispersive model of chromatography

In the mass balance of the simplified equilibrium-dispersive model of chromatography [1], the effects of back-mixing and possible mass transfer limitations are combined into the apparent dispersion coefficient D_{ap}:

$$\frac{\partial C}{\partial t} + F \cdot \frac{\partial q}{\partial t} + u \cdot \frac{\partial C}{\partial x} = D_{ap_i} \cdot \frac{\partial^2 C}{\partial x^2} \quad (3)$$

In this equation the concentrations in the stationary and mobile phases, q and C, respectively, are related through the adsorption isotherm:

$$q = f(C) \quad (4)$$

As both phases are assumed to be in equilibrium, the phase ratio $F = (1 - \epsilon_T)/\epsilon_T$ is based on the total porosity, ϵ_T, representing the liquid fraction in the interstitial space of the column and in the pores of the stationary phase. This porosity is usually determined by measuring the retention time of a non-retained component. The parameter u is the average linear velocity.

Under linear conditions, the apparent dispersion coefficient is related to the number of theoretical plates, N_P, by the equation

$$D_{ap} = \frac{uL}{2N_P} \quad (5)$$

where L is the column length.

In several investigations, this simple model was found to be suitable to describe separations by liquid chromatography [4,11]. Preparative chromatographic columns are packed with particles that are much smaller than those used in large-scale adsorption processes. Hence the more detailed considerations of mass transfer processes in the bed particles which are needed to model these methods and require the inclusion of additional kinetic equations [10] are not necessary in chromatography.

As a consequence of the efficiency of HPLC columns, the boundary conditions (BC) required to solve eqn. 3 can be simplified. Instead of Danckwert's BC for the column inlet, the simple condition

$$C(t, x = 0) = C_E(t) \quad (6)$$

can be used. If a pulse injection is to be simulated, $C_E(t)$ is usually assumed to be a rectangular function. When simulating the FA experiments, consecutive step functions have to be implemented in eqn. 6.

The second boundary condition and the initial condition required to solve eqn. 3 are

$$\left.\frac{\partial C}{\partial x}\right|_{x=L} = 0 \quad (7)$$

The algorithms available for calculating numerical solutions of this problem have been recently reviewed by Katti and Guiochon [1]. For many applications, the very efficient finite difference method proposed by Rouchon *et al.* [11] can be considered as adequate. In this algorithm, the term in eqn. 3 describing the dispersion of the profile is not calculated, but it is simulated by the numerical dispersion of the calculation. This requires selecting the optimum size for the mesh of the (x, t)-grid used in the numerical integration [12].

EXPERIMENTAL

Equipment

The determination of isotherms by FA and the measurement of elution profiles were performed using an HP1090 liquid chromatograph (Hewlett-Packard, Palo Alto, CA, USA), equipped with a temperature-controlled column chamber, a sol-

vent-delivery system, an automatic sample injector, a rapid-scan UV photodiode-array detector and a data station. The detector was calibrated using the plateaux in the FA runs. For a wavelength of 300 nm the slightly non-linear response was fitted with a third-order polynomial for TB concentrations up to 0.005 mol/l.

Materials

Stationary phase. A sample of microcrystalline CTA (15–25 μm) was kindly supplied by Dr. J.N. Kinkel (E. Merck, Darmstadt, Germany). A 10×0.46 cm I.D. stainless-steel column was packed using a slurry technique. Prior to packing, CTA was boiled in ethanol for 30 min to allow its swelling. After cooling and decanting, the suspension was treated in an ultrasonic bath for 5 min at ambient temperature and poured into the packing chamber. An 80-ml volume of ethanol was applied as pushing solvent at a pressure of 275 bar. The work reported in the Part I [13] was carried out with a 25-cm column, which explains some minor differences in the retention factor and adsorption enthalpy.

Following Koller *et al.* [14], the total column porosity was measured by injecting 1,3,5-tri-*tert.*-butylbenzene (TTBB). The retention volume of TTBB varies by less than 2% in the temperature range studied. As it is nearly independent of the temperature within the experimental errors, TTBB can be considered as non-retained on CTA. The results discussed in the Part I [13] show that this is a good approximation. The column efficiency for TTBB was about 400 theoretical plates. The total void volume of the column was 1.0 ml, leading to a total porosity $\epsilon_T = 0.602$. This corresponds to a phase ratio $F = (1 - \epsilon_T)/\epsilon_T = 0.661$.

An additional volume of tubing (0.78 ml) caused a time delay for step injections which were made with the solvent-delivery system, compared with small sample injections made with the automatic sample injector.

Mobile phase and chemicals. All experiments were performed under isocratic conditions, using pure ethanol (100%) from Midwest Grain Products (Weston, MO, USA). Enantiomers of Tröger's base (TB), $C_{17}H_{18}N_2$ ($M = 250.35$ g/mol), with a purity >99.5%, and 1,3,5-tri-*tert.*-butylbenzene were purchased from Fluka (Buchs, Switzerland). All compounds were used as received.

Procedure

The concentration of the solutions used for the FA experiments was chosen to be *ca.* 0.0048 mol/l. The experiments were carried out using the automatic solvent-delivery system to generate the concentration steps. Only steps of increasing concentration were performed for the (−)-enantiomer of TB. Owing to the inflection point observed on the (+)-TB isotherm, several steps with decreasing concentration were also recorded for this enantiomer. The combined analysis of adsorption and desorption steps permits a more accurate determination of isotherms with an inflection point [5,6]. The primary chromatographic data were transferred to the VAX 8700 of the University of Tennessee Computing Center for further processing. The retention time of each concentration front could be determined with a precision better than 1.5%.

Ten concentration steps were performed to determine ten points for each isotherm. The flow-rate in all FA experiments was kept at 0.5 ml/min. Measurements were made at a column temperature of 30, 40 and 50°C for the (−)-enantiomer and at 30°C for the (+)-enantiomer. In addition, elution profiles of small size samples of both TB enantiomers were measured at the same temperatures, to determine the number of theoretical plates according to standard methods, from the retention times and the peak widths [13].

RESULTS AND DISCUSSION

Adsorption isotherms

Fig. 1 shows the FA chromatograms obtained at the three temperatures investigated for the (−)-enantiomer. In Fig. 2 the FA chromatogram of the (+)-enantiomer at 30°C is given.

The equilibrium isotherms obtained for the adsorption of the TB-enantiomers on CTA are shown in Fig. 3. The lines were calculated by fitting the data points to the Langmuir isotherm $[q = q_s b_1 C/(1 + b_1 C)]$ for the (−)-enantiomer and to the quadratic isotherm $[q = q_s C(b_1 +$

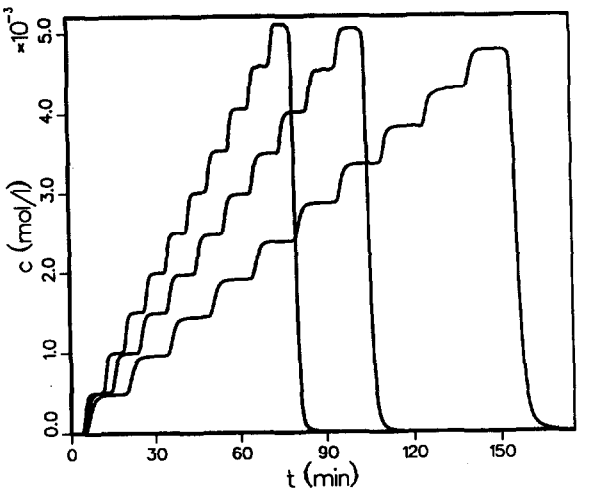

Fig. 1. Frontal analysis to determine the isotherms of the (−)-enantiomer of TB at 30, 40 and 50°C (right to left).

$2b_2C)/(1 + b_1C + b_2C^2)]$ for the (+)-enantiomer. In each case, the selected model describes the experimental isotherm very well. The Langmuir model was not able to account for the (+)-enantiomer isotherm. Although the inflection point is not conspicuous in Fig. 3, its existence has been demonstrated by a series of conclusive results published previously [5,6]. The values obtained for the parameters of the equations and the corresponding standard deviations are given in Table I. These values were calculated by minimizing the following objective function, using Marquard's method [15]:

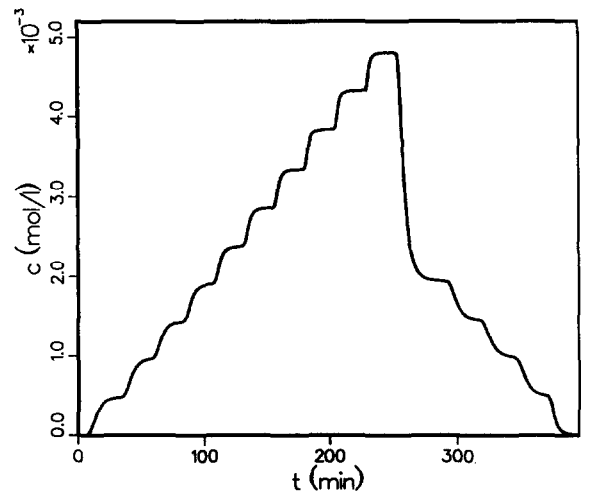

Fig. 2. Frontal analysis to determine the isotherm of the (+)-enantiomer at 30°C.

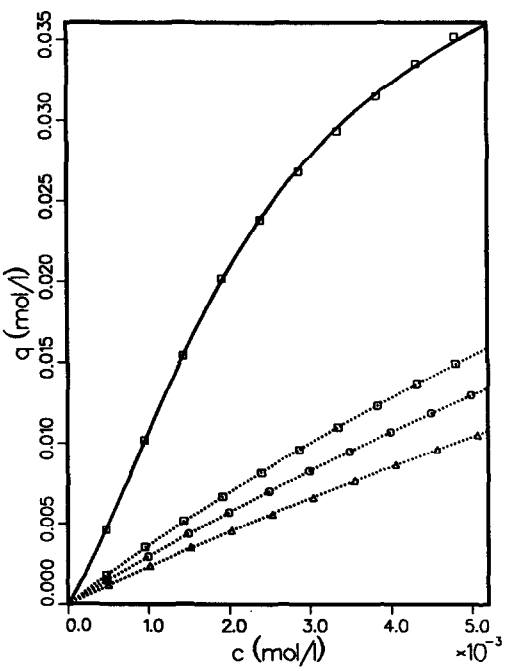

Fig. 3. Isotherms of the (−)-enantiomer of TB on CTA at 30, 40 and 50°C (dotted lines, top to bottom) and of the (+)-enantiomer at 30°C (solid line). The lines were calculated with the Langmuir isotherm for (−)-TB and with the quadratic isotherm equation for (+)-TB, parameters in Table I. The symbols designate the experimental data.

$$\sigma\,(\%) = 100\sqrt{\frac{1}{N_D - P}\sum_{i=1}^{N_D}\left(\frac{q_i^{ex} - q_i^{th}}{q_i^{ex}}\right)^2} \qquad (9)$$

where N_D and P are the numbers of data points and model parameters, respectively.

A thermodynamic analysis of these and addi-

TABLE I

PARAMETERS OF THE ISOTHERM EQUATION (EQN. 2)

Enantiomer	T (K)	q_s (mol/l)	b_1 (l/mol)	b_2 (l²/mol²)	σ (%)
(−)-	303	0.0800	47.6	0	0.50
	313	0.0850	36.0	0	0.28
	323	0.0818	29.2	0	0.79
(+)-	303	0.0239	316.4	173 000	0.65

tional equilibrium parameters for the system TB–CTA–ethanol is given elsewhere [6].

Determination of efficiencies

The unusually broad peaks observed with CTA seriously limit its uses in analytical and preparative chromatography. A detailed study on the influence of solvent composition, temperature and pressure on the efficiency of CTA columns has been performed by Rizzi [16]. The results prove that intraparticle mass transfer processes are the rate-limiting step for separations on CTA. As the apparent dispersion coefficient takes this effect into account, the equilibrium-dispersive model is able to simulate elution band profiles for TB [5].

For preparative purposes, longer CTA columns are necessary to achieve the efficiency required for the separation, and both the temperature and the solvent composition must be optimized carefully. However, as FA requires complete saturation of the stationary phase with the sample, shorter columns are advantageous for the determination of model parameters, as they allow important savings in time and chemicals.

The determination of the apparent dispersion coefficient, or the column efficiency, both linked by eqn. 5, was performed by comparing the theoretical curves generated by numerical solution of eqn. 3 with the experimental fronts. This comparison was done in the range of relevant values of the plate numbers, and gave the best estimate of the plate number. The objective function to be minimized was $OF = \Sigma(c_i^{ex} - c_i^{th})^2$.

Owing to experimental problems, the last two step responses, corresponding to the two highest concentrations studied, were not included in the mathematical analysis. In this range, oscillations of the detector signal were observed (see the second to last or ninth plateau in Fig. 1), and the back-pressure was not stable.

The optimization procedure described above was applied first separately to each of the first eight breakthrough curves, then to the data of all eight fronts together. As grid sizes in the time domain had to be superimposed to minimize *OF*, a linear interpolation of the theoretical values had to be performed to match the times of the experimental data. Another problem was connected with the fact that the algorithm to solve eqn. 3 uses a time grid that is dependent on the theoretical plate number [11]. Since the step functions at the column inlet can be implemented in the numerical scheme only at the grid points, discontinuities appear in the objective function, depending on the plate number. This problem could be circumvented by shifting all experimental step responses in the time scale origin prior to data analysis.

We illustrate the effect of the optimization in Fig. 4 with results obtained in FA of the (−)-enantiomer at 30°C. Shown are the normalized deviations between experimental and theoretical data as a function of time for the first eight fronts. The curves given correspond to 10 (dotted line) and 90 (dashed line) theoretical plates. The plateaux can be recognized as the regions where the deviations between curves almost vanish. The residual errors at these plateaux are mainly due to small calibration errors and to concentration changes in the feed solution due to degassing with helium. Between the plateaux the differences are evident. The value of $N_P = 10$ is obviously too small, as at the beginning of the fronts the concentrations are smaller and at the end of the fronts they are higher than the

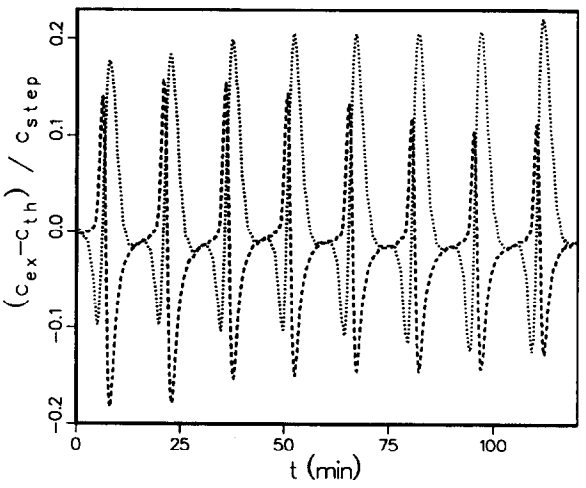

Fig. 4. Differences between experimental and theoretical FA experiment for the first eight steps of the FA experiment with the (−)-enantiomer of TB at 30°C. The dotted line was calculated with 10 and the dashed line with 90 theoretical plates.

theoretical values. The opposite holds for N_P = 90, and this value is too large.

In Fig. 5 we show the results obtained by making the best estimate of the column efficiency as explained above, for four individual fronts and for the data obtained with all eight fronts together. These plots of *OF versus* N_P show a best estimate of the plate number, which increases with increasing solute concentration in the case of the individual fronts.

Fig. 6 summarizes the results obtained as plots, for each four series of FA analysis, of the best estimate of the theoretical plate number *versus* the step rank. The trend observed at 30°C with the (−)-enantiomer, a slow increase in this estimate with increasing concentration, is found also at 40 and 50°C. The plot obtained for the (+)-enantiomer at 30°C is different. It exhibits a sharp minimum at the third step. These differences in mass transfer characteristics between the two TB enantiomers parallel the differences between their adsorption isotherms [5]. The minimum of the number of theoretical plates for the (+)-enantiomer is found at approximately the same concentration as the inflection point of the adsorption isotherm (0.001 mol/l). In agreement with Rizzi [16], the column efficiency for the (+)-enantiomer is only about two thirds of the value for the (−)-enantiomer.

At this point it should be emphasized that in the mathematical analysis performed, the correct isotherms are applied. Therefore, the improved efficiency observed at higher concentrations is not caused by the self-sharpening effect due to a favorably curved adsorption isotherm, but by an actual decrease in the apparent dispersion coeffi-

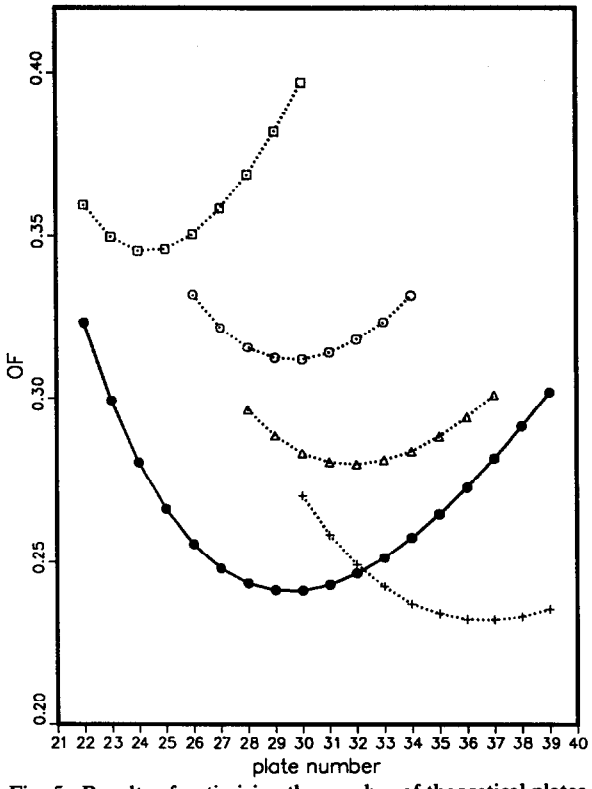

Fig. 5. Results of optimizing the number of theoretical plates for the FA run with the (−)-enantiomer at 30°C. □ = Second front in Fig. 1; ○ = fourth front; △ = sixth front; + = eighth front [in all four cases, *OF* in 10^{-7} $(mol/L)^2$]; ● = all data of the first eight fronts [*OF* in 10^{-6} $(mol/L)^2$].

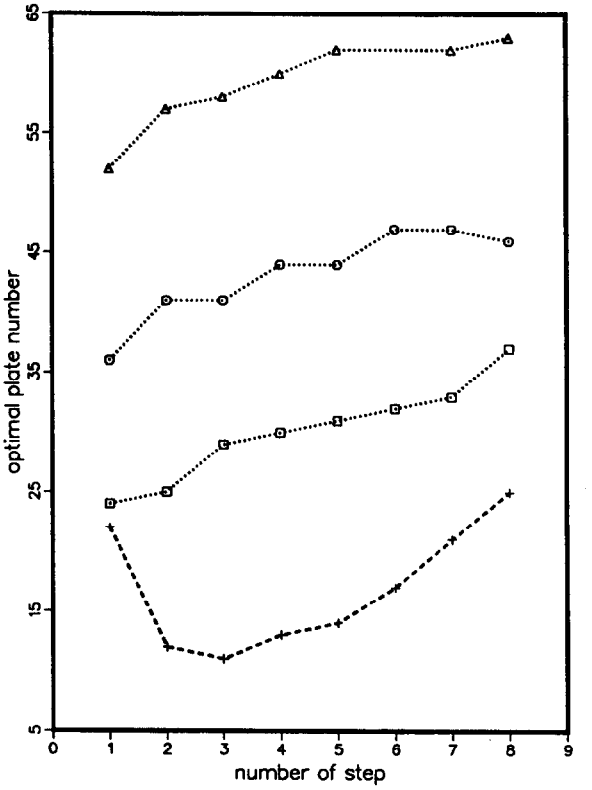

Fig. 6. Dependence of the best estimate of the number of theoretical plates on the rank of the step in the series of FA runs. The step size for each front was 0.00048 mol/l. □ = (−)-enantiomer, 30°C; ○ = (−)-enantiomer, 40°C; △ = (−)-enantiomer, 50°C; + = (+)-enantiomer, 30°C.

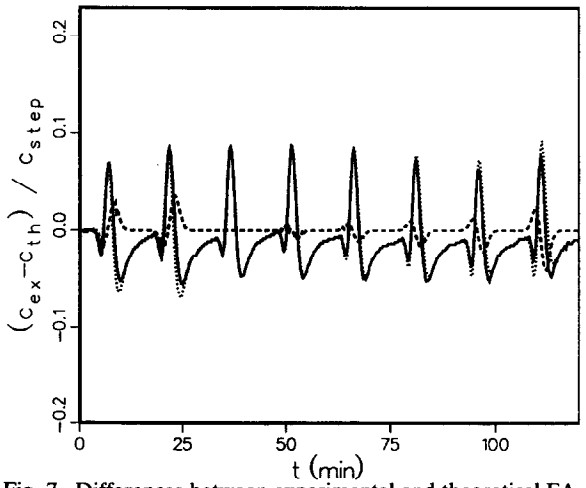

Fig. 7. Differences between experimental and theoretical FA experiments for the first eight steps of the FA experiment with the (−)-enantiomer of TB at 30°C. The solid line was calculated with the best estimate of the number of theoretical plates (see Fig. 5). The dotted line was calculated with the average number of 30 theoretical plates. The dashed line is the difference between the solid and the dotted lines.

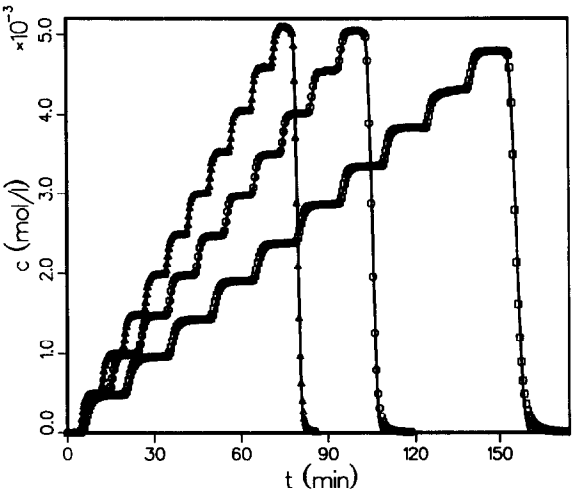

Fig. 8. Comparison between experimental and theoretical FA for the (−)-enantiomer of TB at 30, 40 and 50°C (right to left). The numbers of theoretical plates were 30, 43 and 60, respectively (see Table II).

cient. Whether this corresponds to an increase in the rate of mass transfer is another question.

Fig. 7 shows the deviations between the model and the same experimental data as used in Fig. 4. This time, the solid line was calculated with the best estimate of the theoretical plate number derived for each front, and the dotted line with the average value obtained from optimizing all eight fronts together. The dashed line gives the differences between these two lines. In Fig. 5 it was already clear that the minima are not very pronounced. From Fig. 7, we can conclude that the model used is suitable to describe the adsorption process considered. However, some deviations remain, that could not be eliminated, even when using the optimum values for each individual front. As intraparticle mass transfer is dominant, probably a two-phase model that would take into account the slow transfer in the stationary phase would be able to achieve improved simulations.

Figs. 8 and 9 compare the calculated and experimental FA chromatograms. In the calculations the theoretical plate numbers obtained from optimizing all eight fronts were used. The agreement is excellent. The small deviations in the tail of the desorption fronts of the (−)-enantiomer (Fig. 8) are mainly caused by the presence of a small amount of the longer retained (+)-enantiomer. The agreement appears to be much better in Figs. 8 and 9 than in Fig. 7, because of the smaller concentration scale used.

Thus, in the system studied, the use of a

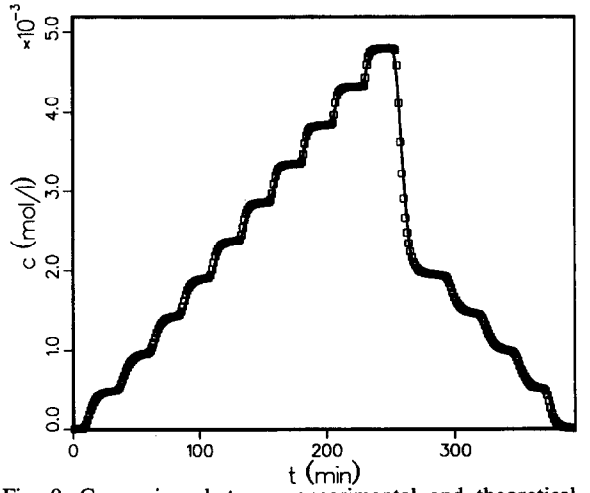

Fig. 9. Comparison between experimental and theoretical FA for the (+)-enantiomer of TB at 30°C. The number of theoretical plates was 16 (see Table II).

constant average mass transfer coefficient seems justified for the calculation of band profiles. However, it should be emphasized again that the increase in the plate number with increasing concentration that we have observed is a real effect. Similar observations were made in analyzing the kinetics of the adsorption of organic components on activated carbon. For the systems studied, a strong increase of the surface diffusion coefficient with increasing loading was reported [17].

In Table II, we compare the numbers of theoretical plates determined as described above by considering together the FA data for all eight fronts, and the values obtained by applying the classical method of evaluating the efficiency of the elution profiles obtained with small size samples. The agreement can be considered as satisfactory.

Finally, from the number of theoretical plates obtained from the elution profiles for the (−)-enantiomer at three different temperatures, it is possible to estimate the activation energy for the apparent dispersion coefficient. We obtain *ca.* 31.5 kJ/mol. This relatively large value is in general agreement with the activation energy of the kinetic parameter k_f discussed in Part I [13]. Axial dispersion, eddy diffusion and intraparticle diffusion processes are known to possess much lower activation energies. As a consequence, it can be concluded that, besides mass transfer resistances, the effect of the kinetics of adsorption–desorption is one of the main contributions to the apparent dispersion coefficient D_{ap}. The latter effect seems to have a dominant influence on the separation of the TB enantiomers on CTA.

TABLE II

NUMBERS OF THEORETICAL PLATES DETERMINED FROM INJECTIONS OF SMALL SIZE SAMPLES (SI) AND FRONTAL ANALYSIS (FA)

Enantiomer	T (K)	N_p(SI)	N_p(FA)
(−)-	303	29	30
	313	44	43
	323	63	60
(+)-	303	20	16

CONCLUSIONS

Our results demonstrate again the importance and usefulness of systematic studies of mass transfer in chromatography under linear conditions and by frontal analysis. These measurements provide an easy access to kinetic data which are useful to understand better the mechanism of the chromatographic process. This is especially useful for separations such as that of the (+)- and (−)-enantiomers of TB on CTA, where poor values of the production rate can be achieved because the positive effect of a high relative retention is offset by slow mass transfer inside the stationary phase.

The concentration dependence of D_{ap} observed during our measurements agrees with previous results [17]. General inclusion of this effect could make the mathematical model much more complicated. However, the concentration dependence seems to be rather inconsequential in the present instance. The use of an average apparent dispersion coefficient, determined from the simultaneous optimization of the data of several fronts, gave results in agreement with the direct determination of the efficiency under linear conditions [13], and calculated profiles in agreement with experimental values. This result validates the use of the equilibrium-dispersive model with a constant apparent diffusion coefficient.

SYMBOLS

b_i	parameter in isotherm equation (eqn. 1) $(l/mol)^i$
C	liquid (mobile) phase concentration (mol/l)
C_0	mobile phase concentration before the step (eqn. 1)
C_E	mobile phase concentration after the step
C_{step}	concentration step for one front in an FA experiment (mol/l)
D_{ap}	apparent dispersion coefficient (m^2/s)
F	phase ratio

L	column length (m)
N_P	number of theoretical plates
N_D	number of data
OF	objective function
P	number of parameters
q	stationary phase concentration (loading) (mol/l)
$q(C_E)$	stationary phase concentration at equilibrium with mobile phase concentration C_E (mol/l)
$q_0 = q(C_0)$	stationary phase concentration at equilibrium with mobile phase composition C_0 (mol/l)
q_S	saturation loading (mol/l)
t	time (s)
t_R	retention time (s)
t_0	retention time of a non-retained component (s)
T	temperature (K)
u	linear velocity, $u = L/t_0$ (m/s)
x	axial coordinate of column (m)

Greek letters

ϵ_T	total porosity
ρ	standard deviation, defined in eqn. 9

Superscripts

ex	experimental value
th	theoretical value

Subscript

E	at column inlet

ACKNOWLEDGEMENTS

We acknowledge the gift of microcrystalline cellulose triacetate and Tröger's base samples by Dr. J.N. Kinkel (E. Merck, Darmstadt, Germany). A.S.-M. is grateful for the support of his stay in Knoxville by the NATO Science Fellowship Program and by the German Academic Exchange Service (DAAD). The HP 1090 liquid chromatograph was a gift from Hewlett-Packard (Palo Alto, CA, USA). This work was supported in part by grant CHE-9201663 from the National Science Foundation and by the cooperative agreement between the University of Tennessee and the Oak Ridge National Laboratory. We acknowledge continuous support of our computational efforts by the University of Tennessee Computing Center.

REFERENCES

1 A. Katti and G. Guiochon, *Adv. Chromatogr.*, 32 (1991) 1.
2 M. Diack and G. Guiochon, *Anal. Chem.*, 63 (1991) 2608.
3 S. Golshan-Shirazi and G. Guiochon, in F. Dondi and G. Guiochon (Editors), *Proceedings of the NATO ASI on Advances in Chromatography and Related Techniques*, Kluwer, Delft, Netherlands, 1992, p. 35.
4 S.C. Jacobson, S. Golshan-Shirazi and G. Guiochon, *AIChE J.*, 36 (1991) 836.
5 A. Seidel-Morgenstern and G. Guiochon, *Chem. Eng. Sci.*, in press.
6 A. Seidel-Morgenstern and G. Guiochon, *J. Chromatogr.*, 631 (1993) 37.
7 E. Francotte and A. Junker-Buchheit, *J. Chromatogr.* 576 (1992) 1.
8 G. Hesse and R. Hagel, *Chromatographia*, 6 (1973) 277.
9 T.L. Hill, *An Introduction to Statistical Thermodynamics*, Addison-Wesley, Reading, MA, 1960.
10 D.M. Ruthven, *Principles of Adsorption and Adsorption Processes*, Wiley, New York, 1984.
11 P. Rouchon, M. Schonauer, P. Valentin and G. Guiochon, *Sep. Sci. Technol.*, 22 (1987) 1793.
12 M. Czok and G. Guiochon, *Comput. Chem. Eng.*, 14 (1990) 1435.
13 S.C. Jacobson, A. Seidel-Morgenstern and G. Guiochon, *J. Chromatogr.*, 637 (1993) 13.
14 H. Koller, K.-H. Rimbock and A. Mannschreck, *J. Chromatogr.*, 89 (1983) 282.
15 D.W. Marquardt, *J. Soc. Appl. Math*, 11 (1963) 431.
16 A.M. Rizzi, *J. Chromatogr.*, 478 (1989) 87.
17 M. Friedrich, A. Seidel and D. Gelbin, *Chem. Eng. Process.*, 24 (1988) 33.